J. Am. Chem. Soc. **1998,** *120,* 10895−10901

Morphology-Dependent Photochemical Events in Aryl Ether Dendrimer Porphyrins: Cooperation of Dendron Subunits for Singlet Energy Transduction

Dong-Lin Jiang and Takuzo Aida*

Contribution from Fields and Reactions, Precursory Research for Embryonic Science and Technology, Japan Science and Technology Corporation, and Department of Chemistry and Biotechnology, Graduate School of Engineering, The University of Tokyo, 7-3-1 Hongo, Bunkyo-ku, Tokyo 113-8656, Japan

Received July 6, 1998

Abstract: A series of dendrimer porphyrins ((L*5*)$_n$P, *n* = 1−4), which bear different numbers (*n*) of five-layered dendron subunits (L*5*) at the *meso*-positions of a porphyrin, were synthesized. Upon excitation of the dendron subunits in CH_2Cl_2 at 20 °C, (L*5*)$_n$P showed an intramolecular singlet energy transfer from the dendron subunits to the porphyrin core, where tetrasubstituted (L*5*)$_4$P with a spherical morphology exhibited a much higher energy transfer quantum yield (Φ_{ENT} = 80.3%) than partially substituted (L*5*)$_1$P−(L*5*)$_3$P (10.1−31.6%). Fluorescence depolarization characteristics of (L*5*)$_4$P indicated that the excitation energy migrates very efficiently over the continuous dendrimeric array of dialkoxybenzyl building units within the lifetime of the excited state. Consequently, the probability of energy transfer to the porphyrin core was enhanced.

Introduction

Dendrimers are hyperbranched, three-dimensional macromolecules with a regular treelike array of branch units.[1] Unlike most synthetic macromolecules of linear chains, they possibly adopt defined (conical and spherical) morphologies in solution. Recently, dendrimeric architectures have attracted increasing attention as artificial antennae for energy transduction,[2,3] as they are morphologically similar to biological light-harvesting antennae.[4] Balzani et al. have reported a tridecanuclear ruthenium(II)−polypyridine supramolecular dendrimer as a light-harvesting complex.[2a,5] More recently, Kawa and Fréchet have reported site isolation and antenna effects on luminescence properties of a self-assembled lanthanide core dendrimer.[2c] On the mechanism of energy transduction, Moore and Kopelman et al. have investigated the fluorescence profiles of a series of perylene-attached dendrons consisting of aromatic and alkynyl units, and they have indicated the importance of an energy gradient for the efficient transfer of the excitation energy.[3a−c] Klafter et al. have also indicated the importance of a geometric bias, inherent to dendrimeric architectures, for energy funneling.[3c,d]

Very recently, we have found that a large, spherical aryl ether azodendrimer traps infrared photons at the dendrimer framework and can channel the excitation energy to the focal point azo unit to cause its *cis/trans* isomerization.[6,7] Interestingly, a nonspherical azodendrimer, in contrast, does not undergo IR-induced isomerization, even though it is sufficiently large. Such a clear morphology dependence of the isomerization of azodendrimers prompted us to investigate “morphology effects” on *excited singlet state* photochemical events in aryl ether dendrimers. In the present paper, we report results of our studies on fluorescence profiles of a series of aryl ether dendrimers having a porphyrin functionality at the focal point ((L*5*)$_n$P, *n* = 1−4; Chart 1) and highlight a morphology dependence of the intramolecular singlet energy transduction.

Results and Discussion

A series of dendrimer porphyrins ((L*5*)$_n$P, *n* = 1−4) having different numbers (*n*) of five-layered aryl ether dendron subunits (L*5*) (Chart 1) were synthesized[8] by Fréchet’s convergent approach[9] and unambiguously characterized by means of MALDI-TOF-MS and ^{1}H NMR. For reference, tetrasubstituted (L*4*)$_4$P[8d] and (L5′)$_4$P[8d] were also synthesized: (L*4*)$_4$P is a one-generation smaller homologue of (L*5*)$_4$P, while (L5′)$_4$P has a nonbranching aryl ether unit between the L4 dendron block and the porphyrin core. A molecular modeling study has predicted a strong preference of tetrasubstituted (L*5*)$_4$P and (L*4*)$_4$P for a spherical morphology,[8d] while partially substituted (L*5*)$_1$P−(L*5*)$_3$P bear “designed” structural defects.

---

* Corresponding author. Phone and fax: +81-3-5802-3363. E-mail: aida@macro.t.u-tokyo.ac.jp.

(1) (a) Fréchet, J. M. J. *Science* **1994**, *263*, 1710. (b) Tomalia, D. A. *Adv. Mater.* **1994**, *6*, 529. (c) Newkome, G. R.; Moorefield, C. N.; Vögtle, F. *Dendritic molecules: Concepts, Syntheses, Perspectives*; VCH: Weinheim, 1996.

(2) (a) Campagna, S.; Denti, G.; Serroni, S.; Ciano, M.; Juris, A.; Balzani, V. *Inorg. Chem.* **1992**, *37*, 2982. (b) Stewart, G. M.; Fox, M. A. *J. Am. Chem. Soc.* **1996**, *118*, 4354. (c) Kawa, M.; Fréchet, J. M. *J. Chem. Mater.* **1998**, *10*, 286.

(3) (a) Devadoss, C.; Bharathi, P.; Moore, J. S. *J. Am. Chem. Soc.* **1996**, *118*, 9635. (b) Kopelman, P.; Shortreed, M.; Shi, Z.-Y.; Tan, W.; Xu, Z.; Moore, J. S.; Bar-Haim, A.; Klafter, J. *Phys. Rev. Lett.* **1997**, *78*, 1239. (c) Bar-Haim, A.; Klafter, J.; Kopelman, R. *J. Am. Chem. Soc.* **1997**, *119*, 6197. (d) Bar-Haim, A.; Klafter, J. *J. Phys. Chem. B* **1998**, *102*, 1662.

(4) (a) Mcdermott, G.; Prince, S. M.; Freer, A. A.; Hawthornthwaite-Lawless, A. M.; Rapiz, M. Z.; Cogdell, R. J.; Isaacs, N. W. *Nature* **1995**, *374*, 517. (b) Kuhlbrandt, W. *Nature* **1995**, *374*, 497.

(5) Balzani, V.; Campagna, S.; Denti, G.; Juris, A.; Serroni, S.; Venturi, M. *Acc. Chem. Res.* **1998**, *31*, 26.

(6) Jiang, D.-L.; Aida, T. *Nature* **1997**, *388*, 454.

(7) Aida, T.; Jiang, D.-L.; Yashima, E.; Okamoto, Y. *Thin Solid Films*, in press.

(8) (a) Jin, R.-H.; Aida, T.; Inoue, S. *J. Chem. Soc., Chem. Commun.* **1993**, 1260. (b) Jiang, D.-L.; Aida, T. *Chem. Commun.* **1996**, 1523. (c) Sadamoto, R.; Tomioka, N.; Aida, T. *J. Am. Chem. Soc.* **1996**, *118*, 3978. (d) Tomoyose, Y.; Jiang, D.-L.; Aida, T.; Yamashita, T.; Horie, K.; Yashima, E.; Okamoto, Y. *Macromolecules* **1996**, *29*, 5236. (e) Jiang, D.-L.; Aida, T. *J. Macromol. Sci., Pure Appl. Chem.* **1997**, *A34*, 2047.

(9) Hawker, G. J.; Fréchet, J. M. J. *J. Am. Chem. Soc.* **1990**, *112*, 7638.

10.1021/ja9823520 CCC: $15.00

Chart 1

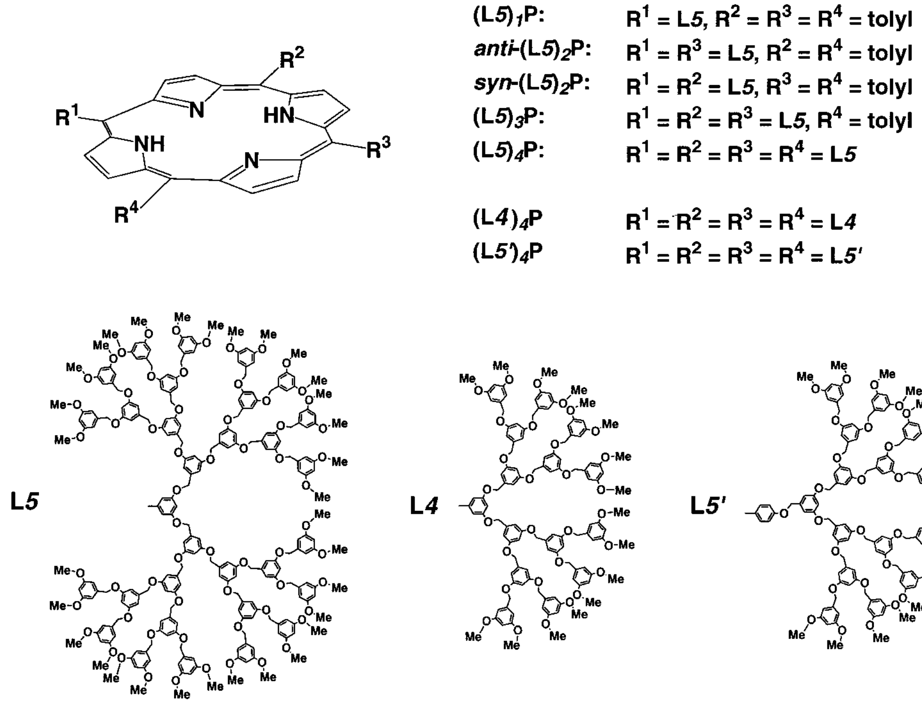

(L5)$_1$P: R^1 = L5, R^2 = R^3 = R^4 = tolyl
***anti*-(L5)$_2$P:** R^1 = R^3 = L5, R^2 = R^4 = tolyl
***syn*-(L5)$_2$P:** R^1 = R^2 = L5, R^3 = R^4 = tolyl
(L5)$_3$P: R^1 = R^2 = R^3 = L5, R^4 = tolyl
(L5)$_4$P: R^1 = R^2 = R^3 = R^4 = L5

(L4)$_4$P R^1 = R^2 = R^3 = R^4 = L4
(L5′)$_4$P R^1 = R^2 = R^3 = R^4 = L5′

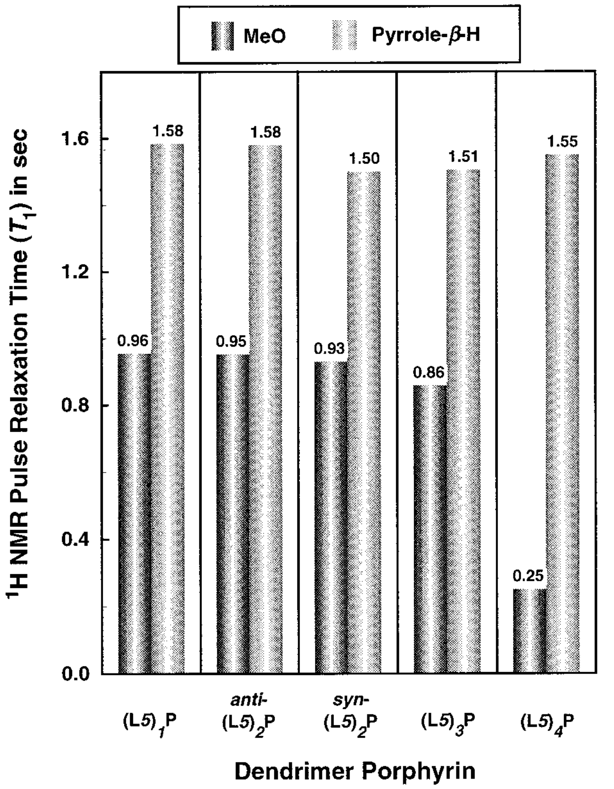

Figure 1. ^{1}H NMR pulse relaxation times (T_1) of MeO and pyrrole-β signals of a series of dendrimer porphyrins (L5)$_n$P ($n = 1-4$) in CDCl$_3$ at 20 °C. T_1 data for (L5)$_4$P are taken from ref 8d.

Figure 1 shows ^{1}H NMR pulse relaxation times (T_1) of (L5)$_n$P ($n = 1-4$) in CDCl$_3$ at 20 °C, which are informative of conformational change dynamics: the T_1 of the pyrrole-β signal of the porphyrin core was virtually unchanged in response to the number of the dendron subunits (n) (1.50−1.58 s), indicating that the interior environment is not constrained even in the largest (L5)$_4$P.[8d] In contrast, the T_1 of the exterior OMe signal, which stayed in the range 0.96−0.86 s at $n = 1-3$, displayed a significant drop (0.25 s)[8d] at $n = 4$. Thus, the dendron subunits in tetrasubstituted (L5)$_4$P are highly constrained in conformation due to their dense packing, whereas those in partially substituted (L5)$_n$P ($n = 1-3$) are able to change their conformation.

Table 1. Electronic Absorption Spectral Profiles of a Series of Dendrimer Porphyrins (L*m*)$_n$P[a]

(L*m*)$_n$P	no. of Ar units in dendrimer subunit	dendrimer subunit		porphyrin core	
		λ_{max}/nm	$\epsilon \times 10^{-5}$ [b]	λ_{max}/nm	$\epsilon \times 10^{-5}$ [b]
(L5)$_1$P	31	280.2	0.9103	421.5	4.9212
anti-(L5)$_2$P	62	280.2	1.8292	422.4	4.9001
syn-(L5)$_2$P	62	280.2	1.8310	422.4	4.8985
(L5)$_3$P	93	280.2	2.7655	424.6	4.7982
(L5)$_4$P	124	280.2	3.6010	425.4	4.6982
(L4)$_4$P	60	280.2	1.8274	424.0	4.7980
(L5′)$_4$P	64	280.2	1.8320	424.0	4.7989

[a] In CH$_2$Cl$_2$ at 20 °C. [b] In M^{-1} cm^{-1}.

Table 1 shows the absorption spectral data of (L5)$_n$P in CH$_2$Cl$_2$ at 20 °C, where the molar extinction coefficient (ϵ) of the absorbance of the dendron subunits increased almost proportionally to n, while the absorption maximum (λ_{max}) stayed at 280.2 nm. On the other hand, the Soret band of the porphyrin core, upon increase in n, slightly red shifted from 421.5 to 425.4 nm (solvatochromism) with a decrease in ϵ (Figure 2), as a result of site isolation of the porphyrin core by the dendrimer framework.[8d] On excitation of (L5)$_n$P in CH$_2$Cl$_2$ at the Soret band of the porphyrin core, all the family emitted fluorescence at 656 and 718 nm, where the intensities were found to be virtually unchanged in response to n when normalized to a constant absorbance at the excitation wavelength. Therefore, the fluorescing property of the porphyrin core is hardly affected by the number (n) of the dendron subunits (no site isolation effect).[10]

---

[10] In ref 8d, we have also shown that the lifetimes of the excited singlet states of a series of tetrasubstituted dendrimer zinc porphyrins [(L*m*)$_4$P]Zn are not affected by the size of the dendrimer framework.

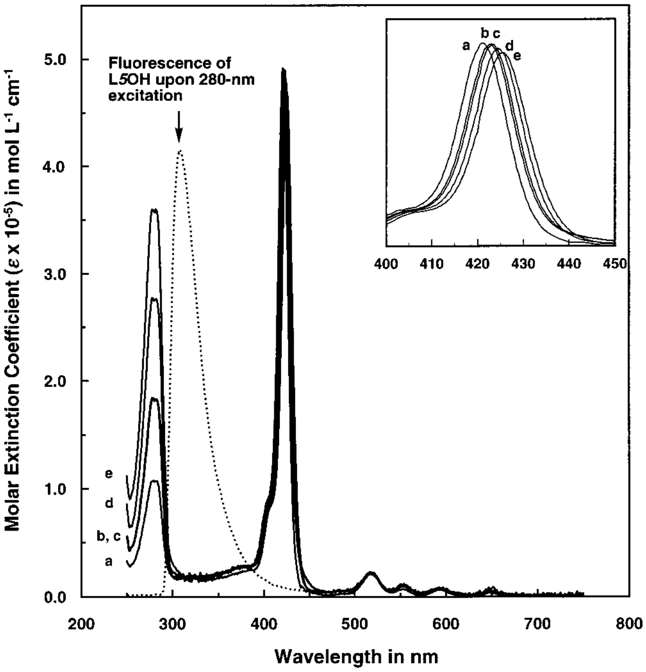

Figure 2. Electronic absorption spectra of a series of dendrimer porphyrins $(L5)_nP$ ($n = 1$ (a), 2 [*anti*] (b), 2 [*syn*] (c), 3 (d), and 4 (e)) in CH_2Cl_2 at 20 °C. The dotted curve represents the fluorescence spectrum of a dendron (L5OH, hydroxyl terminal) upon excitation at 280 nm under Ar in CH_2Cl_2 ($abs_{280\ nm} = 0.02$) at 20 °C.

When a five-layered dendron (L5OH, hydroxyl terminal), equivalent to the dendron subunits in $(L5)_nP$, was excited at its 280-nm absorption band in CH_2Cl_2, it emitted a fluorescence at 310 nm, as shown by the dotted curve in Figure 2. Since the emission is partially overlapped with the Soret absorption band of the porphyrin functionality, the dendron subunits in $(L5)_nP$ have a chance to communicate photochemically with the porphyrin core by energy transfer from the excited singlet state: excitation of the dendron subunits in tetrasubstituted $(L5)_4P$ at 280 nm in CH_2Cl_2 resulted in only a weak emission from the dendron subunits (310 nm) but a strong emission from the porphyrin core (656, 718 nm) (Figure 3e′), where the fluorescence intensity ratio $I_{656\ nm}/I_{310\ nm}$ was as high as 39.4. In sharp contrast, when a 4:1 mixture of the dendron (L5OH) and a non-dendritic porphyrin ($([MeO]_2Ar)_4P$, Chart 2)[11] was excited at 280 nm,[12] the dendron emitted predominantly to furnish a very low $I_{656\ nm}/I_{310\ nm}$ ratio (0.3). Therefore, the strong porphyrin emission, observed for $(L5)_4P$ upon 280-nm excitation (Figure 3e′), is obviously due to an intramolecular singlet energy transfer from the dendron subunits to the porphyrin core (energy trap). The excitation spectrum of $(L5)_4P$, monitored at 718 nm (Figure 4e″), was very similar to the absorption spectrum (Figure 2e), and the energy transfer quantum yield (Φ_{ENT}) was evaluated[13] to be 80.3% (Figure 5).

In sharp contrast to the case of tetrasubstituted $(L5)_4P$, excitation of partially substituted $(L5)_1P-(L5)_3P$ at 280 nm resulted in an emission predominantly from the dendron subunits, with only weak fluorescence from the porphyrin core (Figure 3a′−d′). Figure 4a″ shows the excitation spectrum (monitored at 718 nm) of $(L5)_1P$ having a single dendron subunit, where the relative intensity of the two peaks due to the dendron subunit (280 nm) and the porphyrin core (421 nm) is much smaller than that in the absorption spectrum (Figure 2a), suggesting an extremely low probability of the dendron-to-porphyrin intramolecular singlet energy transfer. In fact, the quantum yield (Φ_{ENT}) of the energy transfer in $(L5)_1P$ was evaluated to be only 10.1% (Figure 5). When the number of the dendron subunits (n) was increased from 1 to 2 (*syn*-$(L5)_2P$) to 3 ($(L5)_3P$), the Φ_{ENT} was also increased in proportion to n (10.1 → 19.7 → 31.6%). However, even $(L5)_3P$ is much inferior to $(L5)_4P$ (80.3%) in terms of Φ_{ENT}, indicating that tetrasubstituted $(L5)_4P$ is a particular one which allows a highly efficient singlet energy transfer from the dendron subunits to the porphyrin core. In relation to this result, *anti*-$(L5)_2P$, a regioisomer of *syn*-$(L5)_2P$, having two topologically separated dendron subunits, showed a low Φ_{ENT} (10.1%), comparable to that of $(L5)_1P$ with a single dendron subunit. Together with this observation, the exceptionally high quantum efficiency of the energy transfer event in tetrasubstituted $(L5)_4P$ indicates a possible cooperation of the four dendron subunits for the singlet

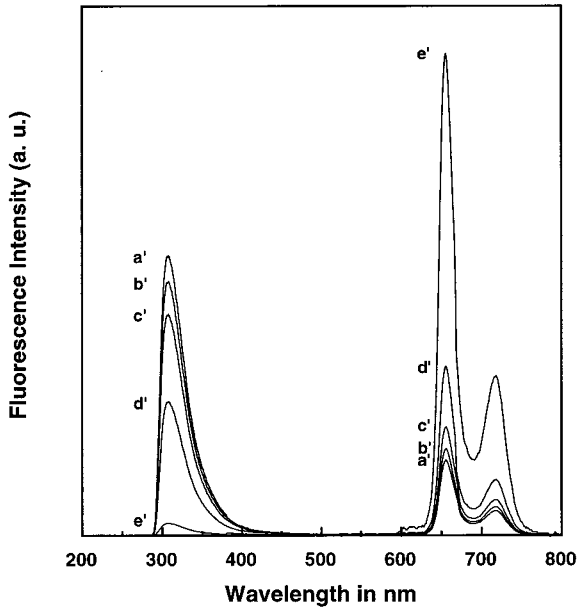

Figure 3. Fluorescence spectra of a series of dendrimer porphyrins $(L5)_nP$ ($n = 1$ (a′), 2 [*anti*] (b′), 2 [*syn*] (c′), 3 (d′), and 4 (e′)), upon excitation at 280 nm in CH_2Cl_2 under Ar at 20 °C. All the spectra are normalized to a constant absorbance (0.02) at the excitation wavelength.

Chart 2

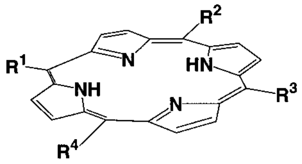

$([MeO]_2Ar)_1P$:	**R^1 = 3, 5-dimethoxyphenyl, $R^2 = R^3 = R^4$ = tolyl**
***anti*-$([MeO]_2Ar)_2P$:**	**$R^1 = R^3$ = 3, 5-dimethoxyphenyl, $R^2 = R^4$ = tolyl**
***syn*-$([MeO]_2Ar)_2P$:**	**$R^1 = R^2$ = 3, 5-dimethoxyphenyl, $R^3 = R^4$ = tolyl**
$([MeO]_2Ar)_3P$:	**$R^1 = R^2 = R^3$ = 3, 5-dimethoxyphenyl, R^4 = tolyl**
$([MeO]_2Ar)_4P$:	**$R^1 = R^2 = R^3 = R^4$ = 3, 5-dimethoxyphenyl**
$([HO]_2Ar)_1P$:	**R^1 = 3, 5-dihydroxyphenyl, $R^2 = R^3 = R^4$ = tolyl**
***anti*-$([HO]_2Ar)_2P$:**	**$R^1 = R^3$ = 3, 5-dihydroxyphenyl, $R^2 = R^4$ = tolyl**
***syn*-$([HO]_2Ar)_2P$:**	**$R^1 = R^2$ = 3, 5-dihydroxyphenyl, $R^3 = R^4$ = tolyl**
$([HO]_2Ar)_3P$:	**$R^1 = R^2 = R^3$ = 3, 5-dihydroxyphenyl, R^4 = tolyl**
$([HO]_2Ar)_4P$:	**$R^1 = R^2 = R^3 = R^4$ = 3, 5-dihydroxyphenyl**

---

[11] UV−vis (CH_2Cl_2): λ_{max} (nm) 421.0, 515.2, 551.5, 589.2, and 644.4.

[12] The absorbance at the excitation wavelength of 280 nm was adjusted to be identical to that of the $(L5)_4P$ solution used for Figure 3e′.

[13] Determined by the method reported in the following: (a) Haugland, R. P.; Yguerabide, J.; Stryer, L. *Proc. Natl. Acad. Sci. U.S.A.* **1969**, *63*, 23. (b) Stryer, L.; Haugland, R. P. *Proc. Natl. Acad. Sci. U.S.A.* **1967**, *58*, 719.

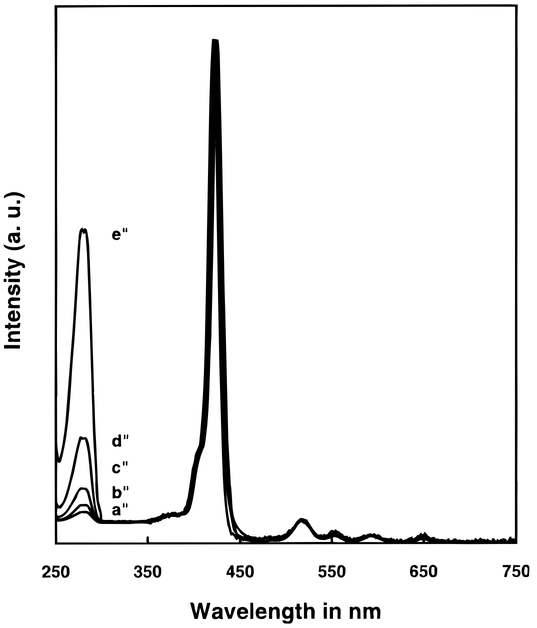

Figure 4. Excitation spectra of a series of dendrimer porphyrins $(L5)_nP$ ($n = 1$ (a″), 2 [*anti*] (b″), 2 [*syn*] (c″), 3 (d″), and 4 (e″)), monitored at 718 nm under Ar in CH_2Cl_2 at 20 °C.

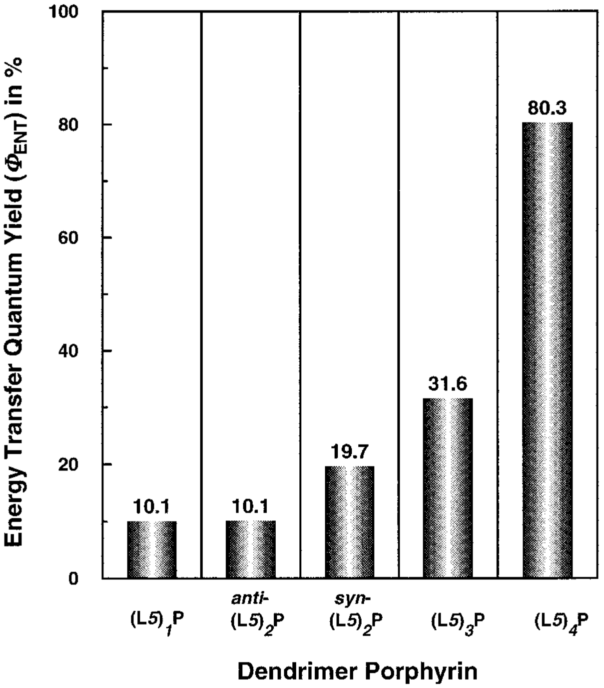

Figure 5. Energy transfer quantum yields (Φ_{ENT}) of a series of dendrimer porphyrins $(L5)_nP$ ($n = 1-4$) upon excitation at 280 nm under Ar in CH_2Cl_2 at 20 °C.

energy transduction. For reference, $(L4)_4P$ (Chart 1), a one-generation smaller homologue of $(L5)_4P$, upon 280-nm excitation, showed a Φ_{ENT} of 79.2%, which is as high as that of $(L5)_4P$ (Figure 5) and much higher than that of *anti*-$(L5)_2P$ (10.1%), having a comparable number of dialkoxybenzyl units (60 versus 62; Table 1). Also interesting is the fact that introduction of a nonbranching aryl ether unit between the L4 dendron block and the porphyrin core ($(L5')_4P$, Chart 1) resulted in a substantial decrease in Φ_{ENT} from 79.2 to 53.7%.

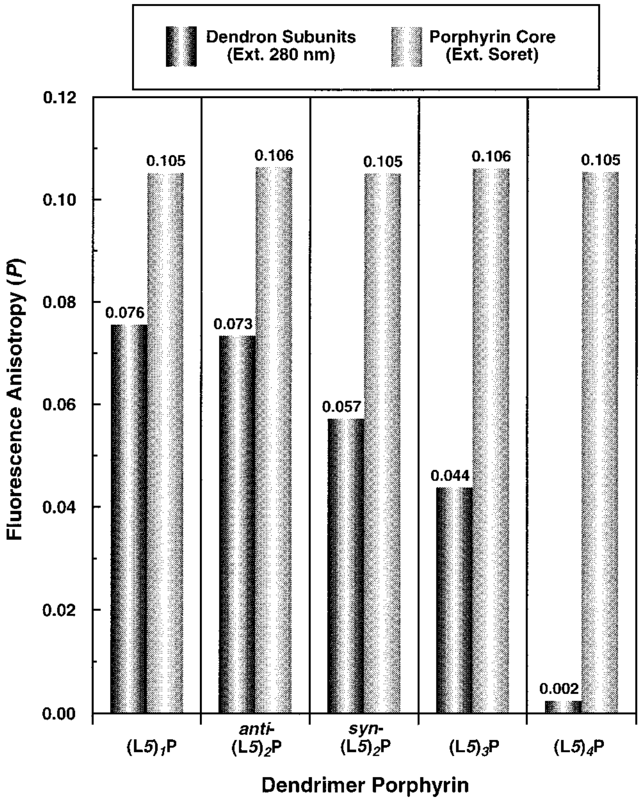

Figure 6. Anisotropies of fluorescences (P) from the dendron subunits (ext 280 nm [abs = 0.02], obsd 310 nm) and the porphyrin core (ext porphyrin Soret [abs = 0.016], obsd 656 nm) in a series of dendrimer porphyrins $(L5)_nP$ ($n = 1-4$) upon excitation with a polarized light under Ar in CH_2Cl_2/polyethylene glycol (MW = 200) at 20 °C. P $(I_{\parallel} - I_{\perp})/(I_{\parallel} + I_{\perp})$, where $I_{\parallel}$ and $I_{\perp}$ represent parallel and perpendicular components of the fluorescence relative to the polarity of the excitation light.

The fluorescence profiles of the dendrimer porphyrins, described above, clearly indicate that the energy transduction event is highly sensitive to the morphology of the dendrimer framework that surrounds the energy trap. For the photochemical event in $(L5)_nP$, we assume that the excitation energy first migrates among the neighboring dialkoxybenzyl (chromophore) units and is then transferred to the porphyrin core (energy trap). Thus, fluorescence depolarization characteristics of $(L5)_nP$ ($n = 1-4$) were investigated upon 280-nm excitation of the dendron subunits with a polarized light, in a viscous medium such as CH_2Cl_2/polyethylene glycol. When a chromophore with a restricted molecular motion is excited by a polarized light, it emits a polarized fluorescence. However, the fluorescence should be depolarized when the excitation energy migrates randomly within the lifetime of the excited state. Here, fluorescence anisotropy (P) is defined by $(I_{\parallel} - I_{\perp})/(I_{\parallel} + I_{\perp})$, using the fluorescence intensities of parallel ($I_{\parallel}$) and perpendicular ($I_{\perp}$) components relative to the polarity of the excitation light. As shown in Figure 6, P was highly dependent on the number of the dendron subunits (n): the fluorescence from the dendron subunits in tetrasubstituted $(L5)_4P$ was considerably depolarized to furnish an extremely low P value (0.002), whereas $(L5)_1P$, with a single dendron subunit, exhibited the highest retentivity of the fluorescence anisotropy ($P = 0.076$) among the family. As for the fluorescences from the porphyrin core via the energy transfer from the dendron subunits, quite similar depolarization profiles were observed, where only $(L5)_4P$ showed an extremely smaller P value (0.002) than those of the rest of the $(L5)_nP$ family ($P = 0.065-0.057$). In sharp contrast, a reference experiment on direct excitation of the porphyrin Soret showed that the depolarization profile of the porphyrin emission was virtually unchanged in response to the number of

Scheme 1. Simplified Schematic Representations of Excited Singlet State Photochemical Events in Aryl Ether Dendrimer Porphyrins of Spherical (A) and Nonspherical (B) Morphologies

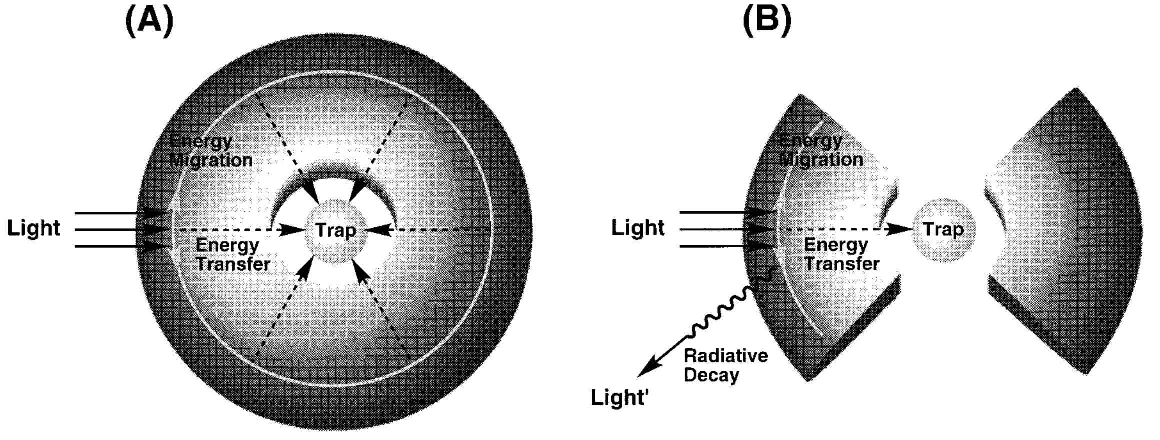

dendron subunits (*n*) (Figure 6). Therefore, the very low *P* values observed for the fluorescences from (L5)$_4$P upon excitation of the dendron subunits indicate the occurrence of an efficient energy migration in the dendrimer framework. In tetrasubstituted (L5)$_4$P, the four dendron subunits appear to behave like a single, large chromophore, where the excitation energy is not localized but can efficiently migrate over the dendrimeric three-dimensional array of the aromatic building units around the energy trap. Consequently, the probability of energy transfer to the interior trap may be highly enhanced (Scheme 1A). On the other hand, in partially substituted (L5)$_n$P ($n = 1-3$), the dendrimeric array of the aromatic building units is much looser and discontinuous, where the energy migration should be less efficient. As the result, most of the excitation energy is lost by radiation before transfer to the energy trap (Scheme 1B).

The cooperativity of the dendron subunits (aromatic building units) for the energy migration process must be reduced upon elevating the temperature to activate conformational motion. Along the line of this idea, we investigated the temperature dependency of the energy transfer event in partially substituted (L5)$_3$P together with those of tetrasubstituted (L5)$_4$P and (L4)$_4$P. When the temperature was raised from 20 to 80 °C in 1,2-dichloroethane, the Φ_{ENT} of (L5)$_3$P upon 280-nm excitation was decreased in a sigmoidal fashion from 31.6 to 12.1% (▲), which is almost comparable to that of (L5)$_1$P, having a single dendron subunit (Figure 7). Tetrasubstituted (L4)$_4$P with one-generation smaller dendron subunits displayed a much clearer temperature dependency, where the Φ_{ENT} dropped significantly from 79.2 to 35.6% (■) on elevating the temperature from 20 to 80 °C. In sharp contrast, the Φ_{ENT} of the largest (L5)$_4$P (●) did not drop but stayed around 80%, even at 80 °C. As already described, the dendron subunits in (L5)$_4$P are highly constrained conformationally, while those in trisubstituted (L5)$_3$P are able to change their conformation rather easily (Figure 1). Tetrasubstituted (L4)$_4$P is almost comparable to (L5)$_3$P in terms of the conformational change activity, considering the ^{1}H NMR T_1 value of the exterior OMe signal (0.81 s).[8d] Since the fluorescing properties of neither the dendron subunits nor the porphyrin core were significantly affected by the temperature in the range 20−80 °C,[14] the clear drops of Φ_{ENT} observed for (L5)$_3$P and (L4)$_4$P at higher temperatures are attributable to a thermally enhanced conformational motion of the molecule: the dendron subunits (aromatic building units) at higher temperatures are likely to behave virtually independently or much less cooperatively for the energy migration process. In this sense, it is quite interesting that the four dendron subunits in the largest (L5)$_4$P are still highly cooperative at 80 °C, indicating a high potential of conformationally rigid, spherical aryl ether dendrimers as artificial antennae for light harvesting.

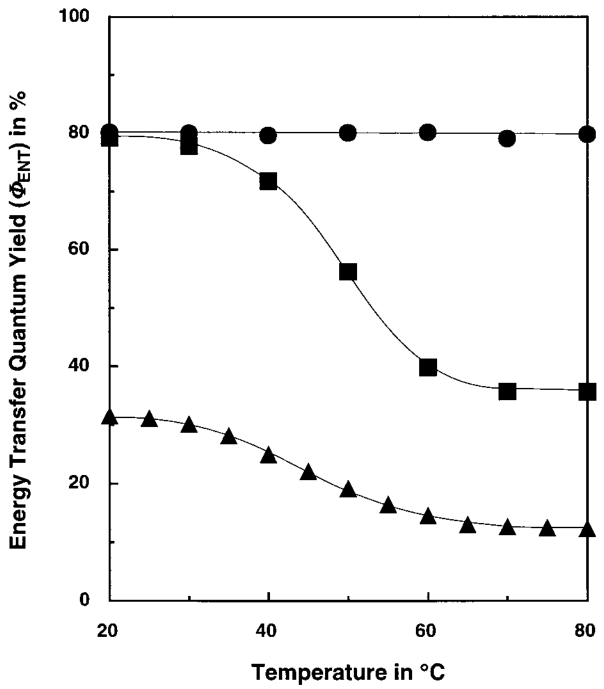

Figure 7. Energy transfer quantum yields (Φ_{ENT}) of dendrimer porphyrins (L5)$_3$P (▲), (L4)$_4$P (■), and (L5)$_4$P (●) at 20−80 °C upon excitation at 280 nm under Ar in 1,2-dichloroethane.

Conclusion

One of the important features of dendrimeric compounds is their defined morphologies, which are hardly expected for linear chain synthetic macromolecules.[15] By taking synthetic and structural advantages of the aryl ether dendrimer porphyrins, we have demonstrated that a spherical dendrimer having a continuous array of chromophores serves as an efficient light-harvesting antenna, where the excitation energy is not localized

---

[14] The fluorescence intensities of L5OH and [(MeO)$_2$Ar]$_4$P in 1,2-dichloroethane remained virtually unchanged on elevating the temperature from 20 to 80 °C.

[15] Webber, S. E. *Chem. Rev.* **1990**, *90,* 1469.

but is able to migrate efficiently over the dendrimeric array of the chromophoric building units that surrounds the energy trap. Consequently, the probability of energy transfer can be enhanced. This observation is interesting in relation to the energy transduction events in wheel-like arrays of chromophores in a purple photosynthetic bacterium,[4] where the excitation energy migrates very rapidly and efficiently along the wheel, followed by transfer to the interior energy trap (special pair) to initiate the photosynthesis. Thus, the present study provides a new strategy for molecular design of light-harvesting materials.

Experimental Section

Materials. Tetrahydrofuran (THF) was refluxed over sodium benzophenone ketyl under Ar and distilled just before use. Dichloromethane (CH_2Cl_2) and 1,2-dichloroethane ($C_2H_4Cl_2$) were refluxed over calcium hydride (CaH_2) under N_2 and distilled before use. Boron tribromide (BBr_3) was used as received (Aldrich). 18-Crown-6 ether was recrystallized from acetonitrile, dried overnight under reduced pressure, and then stored under dry N_2. Potassium carbonate (K_2CO_3) was kept in an oven at 130 °C. Polyethylene glycol (PEG; MW 200) was used as received (Tokyo Kasei). $([MeO]_2Ar)_4P$, $(L5)_4P$, $(L4)_4P$, and $(L5')_4P$ (Charts 1 and 2) were synthesized and unambiguously characterized according to the method reported in our previous paper (see Supporting Information for ref 8d).

$([MeO]_2Ar)_1P$, *anti*-$([MeO]_2Ar)_2P$, *syn*-$([MeO]_2Ar)_2P$, and $([MeO]_2Ar)_3P$ (Chart 2). An acid-catalyzed condensation of 3,5-dimethoxybenzaldehyde, 4-tolualdehyde, and dipyrrylmethane was carried out according to the method reported previously.[16] The reaction mixture was subjected to flash column chromatography on silica gel with CH_2Cl_2 as eluent, where $([MeO]_2Ar)_1P$, *anti*-$([MeO]_2Ar)_2P$, *syn*-$([MeO]_2Ar)_2P$, and $([MeO]_2Ar)_3P$ were isolated as the second, third, fourth, and fifth fractions, respectively.

$([HO]_2Ar)_1P$, *anti*-$([HO]_2Ar)_2P$, *syn*-$([HO]_2Ar)_2P$, and $([HO]_2Ar)_3P$ (Chart 2). $([HO]_2Ar)_1P$. To a dry CH_2Cl_2 solution (10 mL) of $([MeO]_2Ar)_1P$ (0.044 mmol) at -78 °C was added dropwise a CH_2Cl_2 solution (10 mL) of BBr_3 (0.35 mmol) with vigorous stirring under N_2. After 30 min of stirring at -78 °C, the reaction mixture was allowed to stand overnight at room temperature and was poured into ice/water (100 mL), which was then extracted with ethyl acetate (3 × 100 mL). The combined extracts were washed successively with water, brine, and aqueous $NaHCO_3$ and evaporated to dryness after being dried over anhydrous $MgSO_4$. The residue was recrystallized from $CHCl_3$/MeOH to give $([HO]_2Ar)_1P$ (0.042 mmol) as dark purple crystals in 95.4% yield. MALDI-TOF-MS for $C_{47}H_{36}O_2N_4$: *m/z* calcd, 689.81 [MH^+]; found, 689.8. ^1H NMR ($CDCl_3$): δ -2.91 (s, 2H; NH), 2.69 (s, 9H; $ArCH_3$), 6.81 (t, 1H; *p*-H in $C_6H_3(OH)_2$), 7.30 (d, 2H; *o*-H in $C_6H_3(OH)_2$), 7.59 (d, 6H; *m*-H in C_6H_4Me), 8.09 (d, 6H; *o*-H in C_6H_4Me), 8.12 (s, 2H; $Ar(OH)_2$), 8.88 (d, 6H; pyrrole-β-H), 8.95 (d, 2H; pyrrole-β-H).

***anti*-$([HO]_2Ar)_2P$.** To a dry CH_2Cl_2 solution (30 mL) of *anti*-$([MeO]_2Ar)_2P$ (0.026 mmol) at -78 °C was added dropwise a CH_2Cl_2 solution (15 mL) of BBr_3 (0.26 mmol) with vigorous stirring under N_2. The reaction mixture was then treated in a manner similar to that described above, to give *anti*-$([HO]_2Ar)_2P$ (0.025 mmol) as dark purple crystals in 96.1% yield. MALDI-TOF-MS for $C_{46}H_{34}O_4N_4$: *m/z* calcd, 707.79 [MH^+]; found, 707.8. ^1H NMR (acetone-d_6): δ -2.92 (s, 2H; NH), 2.70 (s, 6H; $ArCH_3$), 6.73 (t, 2H; *p*-H in $C_6H_3(OH)_2$), 7.14 (d, 4H; *o*-H in $C_6H_3(OH)_2$), 7.53 (d, 4H; *m*-H in C_6H_4Me), 8.04 (d, 4H; *o*-H in C_6H_4Me), 8.56 (s, 4H; $Ar(OH)_2$), 8.72 (d, 4H; pyrrole-β-H), 8.85 (d, 4H; pyrrole-β-H).

***syn*-$([HO]_2Ar)_2P$.** To a dry CH_2Cl_2 solution (20 mL) of *syn*-$([MeO]_2Ar)_2P$ (0.018 mmol) at -78 °C was added dropwise a CH_2Cl_2 solution (12 mL) of BBr_3 (0.35 mmol) with vigorous stirring under N_2. The reaction mixture was then treated in a manner similar to that described above, to give *syn*-$([HO]_2Ar)_2P$ (0.017 mmol) as dark purple crystals in 94.4% yield. MALDI-TOF-MS for $C_{46}H_{34}O_4N_4$: *m/z* calcd, 707.79 [MH^+]; found, 707.8. ^1H NMR (acetone-d_6): δ -2.89 (s, 2H; NH), 2.58 (s, 6H, $ArCH_3$), 6.71 (t, 2H; *p*-H in $C_6H_3(OH)_2$), 7.12 (d, 4H; *o*-H in $C_6H_3(OH)_2$), 7.52 (d, 4H; *m*-H in C_6H_4Me), 8.01 (d, 4H; *o*-H in C_6H_4Me), 8.57 (s, 4H; $Ar(OH)_2$), 8.74 (d, 4H; pyrrole-β-H), 8.89 (d, 4H; pyrrole-β-H).

$([HO]_2Ar)_3P$. To a dry CH_2Cl_2 solution (50 mL) of $([MeO]_2Ar)_3P$ (0.124 mmol) at -78 °C was added dropwise a CH_2Cl_2 solution (20 mL) of BBr_3 (1.48 mmol) with vigorous stirring under N_2. The reaction mixture was then treated in a manner similar to that described above, to give $([HO]_2Ar)_3P$ (0.116 mmol) as dark purple crystals in 93.5% yield. MALDI-TOF-MS for $C_{45}H_{32}O_6N_4$: *m/z* calcd, 725.76 [MH^+]; found, 725.8. ^1H NMR (acetone-d_6): δ -2.90 (s, 2H; NH), 2.74 (s, 3H; $ArCH_3$), 6.82 (t, 3H; *p*-H in $C_6H_3(OH)_2$), 7.22 (d, 6H; *o*-H in $C_6H_3(OH)_2$), 7.63 (d, 2H; *m*-H in C_6H_4Me), 8.12 (d, 2H; *o*-H in C_6H_4Me), 8.76 (s, 6H; $Ar(OH)_2$), 8.85 (d, 2H; pyrrole-β-H), 9.01 (d, 6H; pyrrole-β-H).

Dendrimer Porphyrins $(L5)_1P$, *anti*-$(L5)_2P$, *syn*-$(L5)_2P$, and $(L5)_3P$ (Chart 1). $(L5)_1P$. A THF solution (35 mL) of a mixture of $([HO]_2Ar)_1P$ (0.014 mmol), L4Br (a four-layered aryl ether dendron bromide; 0.031 mmol), anhydrous K_2CO_3 (0.725 mmol), and 18-crown-6 ether (0.006 mmol) was refluxed under N_2 for 5 days in the dark. The reaction mixture was then evaporated to dryness, and the residue was poured into water (100 mL) and extracted with $CHCl_3$ (3 × 100 mL). The combined extracts were dried over anhydrous Na_2CO_3 and chromatographed on silica gel with $CHCl_3$ as eluent. The third band collected was subjected to flash column chromatography on silica gel with $CHCl_3$ as eluent, and the crude product was recrystallized from CH_2Cl_2/hexane to give $(L5)_1P$ (0.01 mmol) as a purple solid in 71.4% yield. MALDI-TOF-MS for $C_{289}H_{280}O_{62}N_4$: *m/z* calcd, 4800 [MH^+]; found, 4801. ^1H NMR ($CDCl_3$): δ -2.82 (s, 2H; NH), 2.67 (s, 9H; $ArCH_3$), 3.71 (s, 96H; $Ar(OCH_3)_2$), 4.85 (s, 56H; mid and outer Ar-CH_2-OAr′), 5.13 (s, 4H; inner Ar-CH_2-OAr′), 6.34 (t, 16H; *p*-H in $C_6H_3(OMe)_2$), 6.42 (t, 1H; *p*-H in inner C_6H_3), 6.49 (t, 14H; *p*-H in dendron-C_6H_3), 6.58 (d, 32H; *o*-H in $C_6H_3(OMe)_2$), 6.61 (m, 28H; *o*-H in dendron-C_6H_3), 7.21 (d, 2H; *o*-H in inner C_6H_3), 7.52 (d, 6H; *m*-H in C_6H_4Me), 8.07 (d, 6H; *o*-H in C_6H_4Me), 8.83 (d, 6H; pyrrole-β-H), 8.86 (d, 2H; pyrrole-β-H). UV−vis (CH_2Cl_2): λ_{max} (log ϵ) 280.20 (4.9592), 421.50 (5.6921), 515.80 (4.4648), 551.20 (4.1670), 592.50 (4.1361), 651.00 (4.1065).

***anti*-$(L5)_2P$.** A THF solution (10 mL) of a mixture of *anti*-$([HO]_2Ar)_2P$ (0.0021 mmol), L4Br (0.0089 mmol), anhydrous K_2CO_3 (0.106 mmol), and 18-crown-6 ether (0.0018 mmol) was refluxed under N_2 for 10 days in the dark. The reaction mixture was then treated in a manner similar to that described above, to give *anti*-$(L5)_2P$ (0.001 mmol) as a purple solid in 47.1% yield. MALDI-TOF-MS for $C_{530}H_{522}O_{124}N_4$: *m/z* calcd, 8929 [MH^+]; found, 8930. ^1H NMR ($CDCl_3$): δ -2.82 (s, 2H; NH), 2.63 (s, 6H; $ArCH_3$), 3.70 (s, 192H; $Ar(OCH_3)_2$), 4.86 (s, 112H; mid and outer Ar-CH_2-OAr′), 5.12 (s, 8H; inner Ar-CH_2-OAr′), 6.34 (t, 32H; *p*-H in $C_6H_3(OMe)_2$), 6.40 (t, 2H; *p*-H in inner C_6H_3), 6.48 (t, 28H; *p*-H in dendron-C_6H_3), 6.50 (d, 64H; *o*-H in $C_6H_3(OMe)_2$), 6.60 (m, 56H; *o*-H in dendron-C_6H_3), 7.21 (d, 4H; *o*-H in inner C_6H_3), 7.49 (d, 4H; *m*-H in C_6H_4Me), 8.04 (d, 4H; *o*-H in C_6H_4Me), 8.81 (d, 4H; pyrrole-β-H), 8.89 (d, 4H; pyrrole-β-H). UV−vis (CH_2Cl_2): λ_{max} (log ϵ) 280.20 (5.2623), 422.40 (5.6902), 517.10 (4.4626), 552.10 (4.1655), 590.50 (4.1274), 648.40 (4.0060).

***syn*-$(L5)_2P$.** A THF solution (15 mL) of a mixture of *syn*-$([HO]_2Ar)_2P$ (0.014 mmol), L4Br (0.059 mmol), anhydrous K_2CO_3 (0.70 mmol), and 18-crown-6 ether (0.012 mmol) was refluxed under N_2 for 10 days in the dark. The reaction mixture was then treated in a manner similar to that described above, to give *syn*-$(L5)_2P$ (0.008 mmol) as a purple solid in 57.1% yield. MALDI-TOF-MS for $C_{530}H_{522}O_{124}N_4$: *m/z* calcd, 8929 [MH^+]; found, 8931. ^1H NMR ($CDCl_3$): δ -2.82 (s, 2H; NH), 2.63 (s, 6H; $ArCH_3$), 3.69 (s, 192H; $Ar(OCH_3)_2$), 4.85 (s, 112H; mid and outer Ar-CH_2-OAr′), 5.11 (s, 8H; inner Ar-CH_2-OAr′), 6.33 (t, 32H; *p*-H in $C_6H_3(OMe)_2$), 6.39 (t, 2H; *p*-H in inner C_6H_3), 6.46 (t, 28H; *p*-H in dendron-C_6H_3), 6.48 (d, 64H; *o*-H in outer $C_6H_3(OMe)_2$), 6.59 (m, 56H; *o*-H in dendron-C_6H_3), 7.20 (d, 4H; *o*-H in inner C_6H_3), 7.49 (d, 4H; *m*-H in C_6H_4Me), 8.04 (d, 4H; *o*-H in C_6H_4Me), 8.81 (d, 4H; pyrrole-β-H), 8.89 (d, 4H; pyrrole-β-H). UV−vis (CH_2Cl_2): λ_{max} (log ϵ) 280.20 (5.2627), 422.40 (5.6901), 517.10 (4.4625), 552.10 (4.1645), 590.50 (4.1374), 648.40 (4.0160).

---

(16) Tashiro, K.; Konishi, K.; Aida, T. *Angew. Chem., Int. Ed. Engl.* **1997**, *36*, 856.

(L5)$_3$P. A THF solution (35 mL) of a mixture of ([HO]$_2$Ar)$_3$P (0.014 mmol), L4Br (0.086 mmol), anhydrous K_2CO_3 (0.70 mmol), and 18-crown-6 ether (0.01 mmol) was refluxed under N_2 for 20 days in the dark. The reaction mixture was then treated in a manner similar to that described above, to give (L5)$_3$P (0.0068 mmol) as a purple solid in 48.5% yield. MALDI-TOF-MS for $C_{771}H_{764}O_{186}N_4$: *m*/*z* calcd, 13 058 [MH$^+$]; found, 13 061. ^{1}H NMR (CDCl$_3$): δ −2.84 (s, 2H; NH), 2.67 (s, 3H; ArCH$_3$), 3.68 (s, 228H; Ar(OCH$_3$)$_2$), 4.81 (s, 168H; mid and outer Ar-CH$_2$-OAr′), 5.05 (s, 12H; inner Ar-CH$_2$-OAr′), 6.31 (t, 48H; *p*-H in outer C_6H_3(OMe)$_2$), 6.43 (t, 3H; *p*-H in inner C_6H_3), 6.52 (t, 42H; *p*-H in dendron-C_6H_3), 6.56 (d, 96H; *o*-H in C_6H_3(OMe)$_2$), 6.58 (m, 84H; *o*-H in dendron-C_6H_3), 7.01 (d, 6H; *o*-H in inner C_6H_3), 7.51 (d, 2H; *m*-H in C_6H_4Me), 8.01 (d, 2H; *o*-H in C_6H_4Me), 8.79 (d, 2H; pyrrole-β-H), 8.92 (d, 6H; pyrrole-β-H). UV−vis (CH$_2$Cl$_2$): λ_{max} (log ϵ) 280.20 (5.4418), 424.60 (5.6810), 517.10 (4.4561), 552.50 (4.1586), 591.00 (4.1316), 645.50 (4.0160).

Measurements. Electronic absorption spectra were recorded on a JASCO model V-560 spectrophotometer using a quartz cell of 1-cm path length.

Fluorescence and excitation spectra were recorded at designated temperatures, using a quartz cell of 1-cm path length, on a JASCO FP-777W spectrophotometer equipped with a temperature controller and corrected for wavelength-dependent detector sensitivity and excitation light source output. All samples were degassed by five freeze−pump−thaw cycles and purged with Ar just before the measurements. The spectra were normalized to a constant absorbance at the excitation wavelength. Fluorescence anisotropies were measured at 20 °C in CH$_2$Cl$_2$/polyethylene glycol (MW 200) upon excitation of the dendron subunits (280 nm, abs = 0.02) or the porphyrin core (Soret band, abs = 0.016).

^{1}H NMR measurements were performed in CDCl$_3$ or acetone-*d*$_6$ at 21 °C on a JEOL GSX-270 spectrometer operating at 270 MHz, where the chemical shifts were determined with respect to CHCl$_3$ (δ 7.28 ppm) or CH$_3$COCH$_3$ (δ 2.04 ppm). ^{1}H NMR pulse relaxation times (T_1) were measured in a saturation recovery data processing mode.

Matrix-assisted laser desorption ionization time-of-flight mass spectroscopy (MALDI-TOF-MS) was performed on a Bruker model ProteinTof mass spectrometer using 9-nitroanthracene (9NA) as a matrix.

Acknowledgment. D.L.J. thanks the JSPS Young Scientist Fellowship.

JA9823520